

Measuring the linearity of X-ray detectors: consequences for absolute attenuation, scattering and absolute Bragg intensities

Zwi Barnea,^{a*} Christopher T. Chantler,^a Jack L. Glover,^{a,b} Mark W. Grigg,^d M. Tauhidul Islam,^{a,e} Martin D. de Jonge,^c Nicholas A. Rae^a and Chanh Q. Tran^f

^aSchool of Physics, University of Melbourne, Australia, ^bNational Institute for Standards and Metrology, Gaithersburg, Maryland, USA, ^cAustralian Synchrotron, Clayton, Australia, ^dDefence Science and Technology Organization, DSTO Fairbairn, Canberra, Australia, ^eSchool of Chemistry, University of Melbourne, Australia, and ^fDepartment of Physics, La Trobe University, Australia. Correspondence e-mail: barnea@physics.unimelb.edu.au

The linearity of response of X-ray detectors is tested. Examples of linearity tests demonstrate the remarkable range of linear response of flowing-gas ion chambers in the synchrotron environment. The diagnostic is also highly sensitive to the presence in the X-ray beam of harmonic X-rays diffracted by a higher-order reflection of the monochromator. The remarkable range of linearity of ion chambers has enabled the accurate measurement of the absolute X-ray attenuation of a number of elements. It should now be possible to measure the absolute intensity of Bragg reflections, provided such measurements are carried out with extended-face single crystals. The advantages of the extended-face crystal technique for Bragg intensity measurements are summarized and a number of approaches to absolute Bragg intensity measurement are discussed.

© 2011 International Union of Crystallography
Printed in Singapore – all rights reserved

1. Introduction

Nonlinearities in (X-ray) detector response with incident flux or intensity are prevalent in many of our standard experiments using laboratory or synchrotron sources. Where unnoticed, they distort measured relative intensities, derived structures, temperature parameters and bonding interpretation.

A number of papers have recognized the serious nature of the issue and observed the consequences of nonlinearities in experiments with various X-ray detectors. Photographic emulsions, X-ray or otherwise, have been used and investigated since the discovery of X-rays. Careful studies of the linearity of the dose–response function have resulted; these have been accompanied by the development of special-purpose films, and the comparison of nonlinearities of UV–vis emulsions and X-ray emulsions has been a continuing interest (Dozier *et al.*, 1967; Henke *et al.*, 1984). The dose–response function is based around cluster statistics and is highly nonlinear (Chantler, 1993; Chantler *et al.*, 1993). In this case the nonlinearities are dramatic so must be modelled carefully, but while the form and nature of nonlinearities is now well understood, the characterization of a particular film is complex and rarely attempted. Nonetheless the high resolution and stability of photographic emulsions mean that they have only recently being overtaken by electronic pixelated detectors, and major results using X-ray films and corrected for their nonlinearities are still being published (Grigg & Barnea, 1996; Chantler *et al.*, 2007, 2009).

Electronic systems rapidly expanded to applications for X-ray detection, for which they are especially suited given

their tuneability with energy by selecting appropriate gas types and pressures. Some of the early work demonstrated strong nonlinearities, especially near saturation, due to ion-pair production, dead layers, recombination and other factors (Chantler & Staudenmann, 1995). Importantly, the design of ion chambers and optimization of electronics and intensity settings can minimize these nonlinearities (*e.g.* Tran *et al.*, 2003). While ion chambers and scintillators have dominated scanning geometries, imaging plates have come to dominate full-field crystallographic data collection, largely because the simultaneous collection provides a temporal normalization of the signals. Nevertheless, imaging plates can be strongly nonlinear across ranges of energies and fluxes; also, care must be taken with readout times as the signal fades within periods of the order of several hours (Cookson, 1998). Similarly, two-dimensional backgammon detectors must be calibrated spatially and in relative intensities to achieve accurate data (Payne *et al.*, 2009, 2010), and even relatively modern avalanche photodiodes have shown strong quadratic (*i.e.* highly nonlinear) response functions to flux, affecting the interpretation of Young's double-slit experiments and requiring calibration before reliable interpretation can be made (Paterson *et al.*, 2001).

In summary, all detectors have potential nonlinearities; assessing and correcting for these is a prerequisite for accurate interpretation of X-ray intensities and their uncertainties, and hence for the consequent reliability of the results, such as absorption coefficients or derived crystal structures. Most of the above studies have observed discrepancies that were

interpreted as detector nonlinearities and then corrected, usually by modelling; however, it is preferable to characterize the response function directly.

Investigating the linearity of response of X-ray detectors or X-ray counters and their associated electronics to incident flux thus constitutes an essential preliminary task in any measurement of X-ray intensities. Such tests are particularly important in the synchrotron environment, where X-ray beam intensities are extremely high and their measurement may therefore be severely affected by nonlinear response of the detector and its associated counting chain.

To test the linearity of response of a detector, the intensity of the X-ray beam needs to be varied in a known manner over the intensity range of interest and the response to this variation determined. In the case of count-rate meters, such as for example proportional and scintillation counters, ion chambers, or solid-state position-sensitive detectors, the intensity can be

readily varied by attenuating the X-ray beam with known thicknesses of foil. In the case of dose-measuring media, such as for example imaging plates, a well defined variation of the X-ray dose can also be achieved by varying the exposure time of the medium to an X-ray beam of constant intensity, the response being linear as long as the recorded count is proportional to the exposure time (see §4).

2. Examples of linearity tests

Examples of linearity tests performed on a flowing-nitrogen ion chamber using multiple aluminium foils of equal thickness as absorbers of monochromated synchrotron beams of various energies are shown in Fig. 1. Here the foil-attenuated intensity I is given by

$$I = I_0 \exp[-(\mu/\rho)(\rho t)], \tag{1}$$

where I_0 is the incident X-ray beam intensity, μ/ρ is the X-ray mass absorption coefficient of aluminium for the energy of the X-ray beam and t is the thickness of the foil. In Fig. 1 the negative values of the natural logarithms of the measured ratios of I/I_0 ,

$$-\ln(I/I_0) = [(\mu/\rho)(\rho t)] = \mu t, \tag{2}$$

are plotted as a function of the number of aluminium absorbers. The fact that the values of $\ln(I/I_0)$ plotted against t fall on a straight line with slope μ attests to the rather remarkable range of linear response of the ion chamber and its associated counting chain, when optimized, for a range of measured intensities starting with I_0 , the full monochromated unattenuated synchrotron X-ray beam, down to the lowest intensity I measured. The number of foils in Fig. 1 covers a factor of 250 in thickness variation but, as demonstrated in Fig. 2, the attenuation covers in excess of $\exp(11)$ or five decades in the ratio of the intensities I and I_0 that can be measured within the linear response range of the counting system – a ratio entirely sufficient for the absolute measurement of attenuation. The uncertainties in the data points are much smaller than the dots and are, for example, 0.24, 0.21 and 0.28% for the most

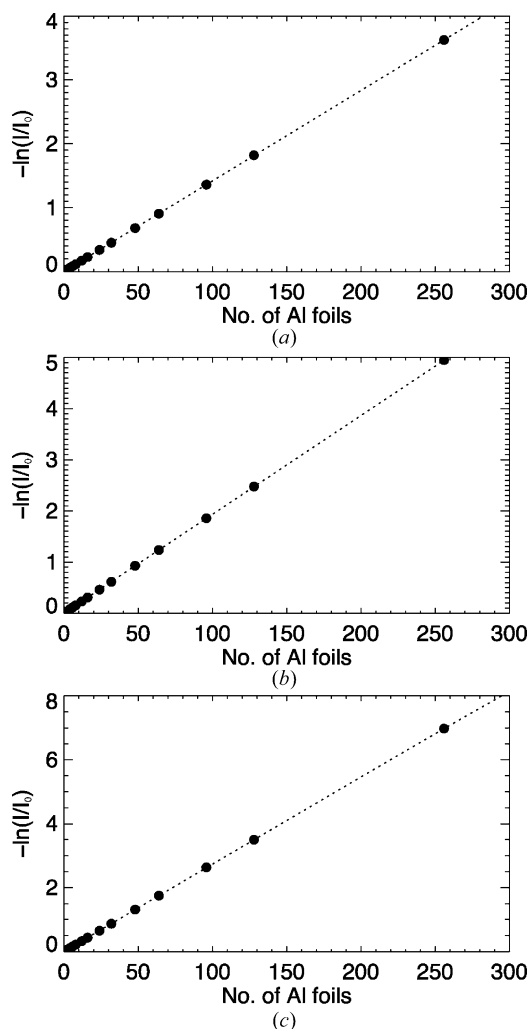


Figure 1
Plots of $-\ln(I/I_0)$ as a function of the number of absorbing aluminium foils at three X-ray energies, demonstrating the large range of linearity of the detector response to the intensity and flux in the downstream ion chamber. Uncertainties in measured signal allow for background subtraction and are much smaller than the size of the dots. (a) Measured linearity for 20 keV X-ray fluxes at ANBF, Tsukuba, Japan; (b) 18 keV; (c) 16 keV.

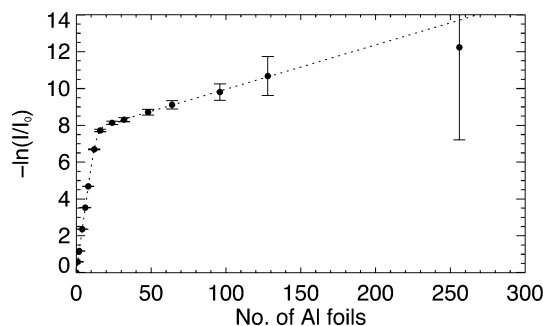


Figure 2
Plot of $-\ln(I/I_0)$ as a function of the number of absorbing aluminium foils at 5.407 keV, demonstrating the presence of 0.038 (2)% harmonic radiation diffracted by the (333) planes of the silicon monochromator at 16.22 keV (*i.e.* 3×5.407 keV). This gives a very clear signature with the second observable slope corresponding to the absorption coefficient for the (third) harmonic energy, when the primary energy is fully absorbed.

sensitive points with 250 thicknesses at the three energies 20, 18 and 16 keV, respectively. This includes allowance for non-uniformities and impurities. The accuracy of the observed linearity is perhaps best appreciated by considering Fig. 2, where a mere 0.038% of radiation has a photon energy three times that of the fundamental monochromated beam. Hence the nonlinearity equivalent to a harmonic contamination in the plots of Fig. 1 is clearly less than 0.038%. For comparison, examples of nonlinear response can be seen, for instance, in Fig. 3 below and in the work of Grigg & Barnea (1996).

When producing the linearity plots we corrected all our intensity measurements for the intensity variation of the synchrotron X-ray beam, which was monitored throughout by a matched flowing-nitrogen monitor ion chamber located upstream of the absorbing foils, as well as for the ion-chamber dark current (*i.e.* the counts recorded with the X-ray beam off).

Since we used multiple layers of foil to attenuate the beam, we assumed that the inevitable small local differences in foil thickness would average out. It is, of course, possible first to determine accurately the attenuation of each individual foil at the point of the foil through which the beam actually passes, although we did not consider this necessary for our measurement accuracy. The multiple foils were mounted on the rim of a daisy wheel, which allowed for easy insertion of the various thicknesses by a remotely controlled rotation of the daisy wheel.

Fig. 2 shows a similar linearity test at 5.407 keV, where in spite of optimal detuning of the monochromator (Beaumont & Hart, 1974; Bonse *et al.*, 1976) a minute residual fraction of harmonic radiation is shown to be present in the beam. Here the upper part of the curve in particular demonstrates graphically the presence of the higher-order radiation, while

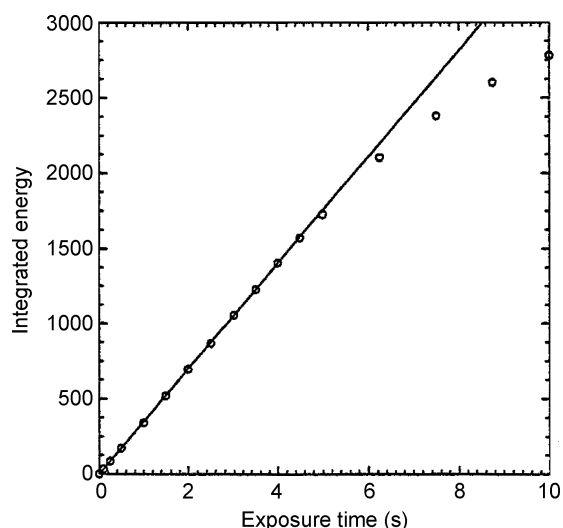


Figure 3 Imaging plate response after summation of all pixels within the direct-beam image area. The same area was used for each summation, and the averaged background has been subtracted. This demonstrates linearity and deviation from it with flux (exposure integrated over time) as opposed to comparing different intensities incident in a given period of time, as presented in Figs. 1 and 2

the entire curve attests to the range of linearity. The use of this technique to detect and determine the presence of the harmonic fraction in a monochromated beam has been discussed in detail elsewhere (Barnea & Mohyla, 1974; de Jonge *et al.*, 2004; Tran, Chantler *et al.*, 2004); we include the figure here as an example of a highly useful by-product of linearity testing. Note especially that this test covers over exp(11) in attenuation or over five decades of detector linearity, which is a range of linearity sufficient for the direct absolute measurement of scattering cross sections and intense Bragg reflections (see also §4).

It is worth emphasizing that linearity must be tested over the entire range of measured X-ray intensities and energies. When the X-ray source is a synchrotron, this means that to include the highest intensities such a test must be carried out at the beginning of the synchrotron cycle when beam intensities are greatest and in the entire range of energies to be included in the experiment.

3. Absolute intensity measurements

So far we have used the above linearity tests mostly in the course of absolute intensity measurements of the X-ray attenuation, including measurements in the XAFS region (*e.g.* de Jonge *et al.*, 2005, 2007; Glover *et al.*, 2008; Islam *et al.*, 2010; Rae *et al.*, 2010), using a suite of techniques collectively referred to as the X-ray extended range technique, which makes it possible to measure X-ray absorption down to an accuracy of better than 0.05%. There is, however, considerable further scope for absolute X-ray intensity measurements that can be applied to other interesting problems, in particular to the absolute measurement of integrated Bragg intensities, whose great importance was recognized very early (see, for example, Bragg & West, 1928; Lipson & Cochran, 1957).

When we refer to absolute measurements, we follow the early definition of such measurements by Bragg & Bragg (1962): ‘An absolute measurement is a comparison of the diffracted beam with the incident radiation, a ratio which has an important theoretical significance.’ The total energy E diffracted by an ideally imperfect (mosaic) extended-face crystal is given by James (1962) and Warren (1969) as

$$E = \frac{P_0}{\omega} \left(\frac{e^4}{m^2 c^2} \right) \frac{\lambda^3 F_T^2}{2\mu V_a^2} f_{Lp}, \quad (3)$$

where the power of the incident beam $P_0 = A_0 I_0$ and A_0 is the cross-sectional area of the incident beam, ω is the angular rate at which the crystal is rotating through the Bragg angle, e and m are the electron charge and mass, c is the speed of light in vacuum, λ is the wavelength of the X-rays, F_T is the structure factor including the effects of thermal motion, V_a is the volume of the unit cell, f_{Lp} is the Lorentz–polarization factor, and μ is the linear X-ray absorption coefficient. The extended-face single crystal is assumed to be sufficiently thick not to transmit any of the incident beam. The diffraction is from the flat face of the crystal (this is the Bragg geometry). The

absorption correction in this case is given by the factor $1/(2\mu)$ in equation (3).

The principal difficulty in measuring E and P_0 arises from the very substantial differences in the intensities of the incident and diffracted beams, which for ideally imperfect crystals differ by a factor of between about 10^4 and 10^6 (e.g. Grigg, 1994) and require an X-ray detector response linear over such a range (as can be reached by ion chambers).

The other difficulty in the measurement of absolute Bragg intensities is encountered when employing the almost universal technique of small single crystals bathed in the incident X-ray beam. The chief obstacle then is the extreme difficulty of separating and measuring the intensity of that part of the incident beam intercepted by the diffracting crystal, as well as in allowing accurately for the absorption of the X-rays by the crystal. Fortunately this difficulty can be easily avoided in those instances when large single crystals are available.

We have demonstrated repeatedly the remarkable advantages of using extended-face imperfect crystals for accurate measurement of relative X-ray integrated Bragg intensities even in the case of very highly absorbing crystals (Harada *et al.*, 1970; Mair *et al.*, 1971; McIntyre *et al.*, 1980; Stevenson & Barnea, 1983a, 1984; Stevenson *et al.*, 1984; Stevenson, 1994). Briefly, these advantages include the following:

(1) An extremely simple absorption factor and an uncomplicated geometry resulting in high consistency of measured integrated intensities as attested by the agreement of equivalent reflections.

(2) High diffracted intensities as a result of the utilization of the fully intercepted incident X-ray beam.

(3) Ready access to a large portion of reflections in half of the limiting sphere from a single extended crystal face without the need to modify diffractometer control software.

(4) Special advantages when measuring Bijvoet pairs of reflections in noncentrosymmetric crystals.

(5) The ability to control and characterize the preparation of the flat extended crystal face.

(6) The possibility of absolute intensity measurement (Grigg, 1994; Barnea *et al.*, 2010).

It is the last of these that is of principal interest in the present context. In the extended-face crystal technique the flat face of a single crystal intercepts the entire incident X-ray beam. Given a detector with a sufficient range of linear response, it is therefore possible to compare the diffracted integrated Bragg intensities directly with the intensity of the incident X-ray beam, determine the absolute integrated intensity of one or more reflections, and proceed to investigate a new series of highly interesting problems.

Just to cite some examples, by no means a complete list, measurements of absolute Bragg intensities are essential when comparing observed extinction effects with theory because they avoid the problems due to the high correlation between the refined scale factor and extinction constants, which is inevitable when comparisons are made employing relative intensities.

The observed extinction effects essentially follow the predictions of the theory of Zachariasen (1967) with the

effective domain radius $r^* = r \sin 2\theta$, where the $\sin 2\theta$ factor is a correction suggested by Becker & Coppens (1974a,b). We note that, in the case of reflections with very severe extinction, this theory overcorrects the intensities, as shown in the extended-face crystal measurements of ZnSe (Stevenson & Barnea, 1983b) as well as in GaAs (Stevenson, 1994); this is a problem that requires further study.

Eventually, reliable absolute Bragg intensities and the resulting understanding of extinction may make it possible to directly measure atomic form factors as well as dispersion effects and their energy dependence. This is of great interest in the vicinity of the K -absorption edges where disagreement between observed and calculated Bijvoet ratios has been observed (Stevenson & Barnea, 1983b; Barnea *et al.*, 2010). It is also in this region that differences between tabulated and measured X-ray absorption coefficients, and hence discrepancies of the imaginary part of the dispersion corrections, have been repeatedly reported (de Jonge *et al.*, 2005, 2007; Rae *et al.*, 2010).

It should now also be possible to determine the absolute intensity of forbidden reflections and even of diffuse and other types of scattering (Chantler *et al.*, 2001; Tran, de Jonge *et al.*, 2004), to obtain reliable data on bonding, thermal effects and anharmonicity, as well as to establish the absolute fluorescent radiation yield. Knowledge of absolute X-ray intensities is fundamental for establishing X-ray standards and will be useful in medical applications and practice.

The linear response of the counter and counting chain is particularly important when measuring high Bragg intensities. The effect of nonlinear response is greatest for the most intense reflections and may therefore be impossible to separate from the effects of extinction.

We should also stress here the importance of the X-ray linear absorption coefficient, an accurate value of which is required for determining the absolute integrated Bragg intensity [*cf.* equation (3)]. Our measurements of absorption and attenuation coefficients demonstrate that these coefficients can differ appreciably from their various tabulated values, particularly in the important and interesting region of the K -absorption edge.

4. An alternative approach using imaging plates

It is instructive to consider for comparison an alternative approach to measuring absolute intensities employing, for example, imaging plates – a dosage measurement medium.

The response of imaging plates to X-rays is nonlinear and the digitization is generally logarithmic. With suitable caveats and calibration, the digitized pixel value is the logarithm of the imaging-plate signal so that an exponential of the digitized signal with a suitable offset term (Cookson, 1998) approximates a linear response within a range of incident flux. The conversion of the digitized readout signal to a linear response over the given range can be carried out by suitable readout software.

Fig. 3 shows a plot of increasing exposure times to the integrated energy of a monochromated molybdenum $K\alpha$

beam from a stabilized laboratory X-ray source. The range of linearity is about 10^3 , in good agreement with the 5×10^3 linearity range reported by Miyahara *et al.* (1986). This relatively modest linearity range is insufficient to bridge the gap between the direct and integrated diffracted intensities, which differ by a factor of about 3×10^4 through 10^7 if we are also to include stronger reflections from perfect crystals (Chantler, 1992*a,b*; Grigg, 1994).

However, this gap between the direct-beam intensity and the diffracted beams can be narrowed by a number of techniques:

(1) By attenuation of the direct beam with a calibrated attenuator.

(2) By shortening exposures to the direct beam and extending exposures to the diffracted beam.

(3) By using timed exposures to establish the linearity of response of the imaging plates accurately (Fig. 3).

(4) By introducing a narrow slit between the direct beam and the counter and carrying out a narrow-aperture 2θ scan across the direct beam. This can be combined with detection by a moving imaging plate (item 5 below).

(5) By rotating and/or translating the imaging plate during exposure to the direct beam in order to spread the footprint of the direct beam over a larger area of the plate.

(6) In the case of laboratory X-ray sources, by decreasing the tube current when measuring the direct beam and increasing it when measuring the diffracted beam.

(7) Another possible technique for expanding the range of linear response applies both to dose and to rate-meter detectors and involves the splicing of two detectors whose intensity regions of linear response partially overlap. Where such an overlap does not exist, it can be achieved by introducing into the incident beam a suitably calibrated absorber when measuring with the detector whose range of linear response occurs at lower X-ray intensities. This has the effect of shifting its linearity response range toward higher X-ray intensities, causing it to overlap with the second detector.

Each of these techniques has, of course, advantages and drawbacks. In an exploration of methods of absolute intensity measurement Grigg (1994) used the first four of the above techniques to determine the absolute integrated Bragg intensities of three reflections of cadmium sulfide whose crystal structure, thermal motion and anharmonicity had previously been determined from relative intensities measured by the extended-face crystal technique (Stevenson *et al.*, 1984).

Comparison of the results Grigg obtained with a film-CCD counter combination, with imaging plates and with two counter techniques showed a pleasing consistency of the absolute intensity to within about 1.5%. Interestingly, for molybdenum characteristic radiation, the various tabulated cadmium sulfide absorption coefficients differ by about 3% (Creagh, 1999; Chantler, 1995*a,b*). In the present uncertain state of the tabulations, absolute measurement of Bragg intensities therefore requires one also to measure the linear absorption coefficient.

The subtraction of background from the Bragg reflection during absolute intensity measurements is better carried out

by employing a counter technique (McIntyre, 1981) than by the use of dosage-measuring media.

5. Conclusion

We have demonstrated the remarkable range of linear response of ion chambers to X-rays in the synchrotron environment. The linearity tests are also shown to be highly sensitive to harmonics present in the X-ray beam. The range of linear response of ion chambers is probably sufficient to allow absolute measurements of intense Bragg reflections relative to the incident X-ray beam intensity when using extended-face single crystals. Some applications of such measurements have been discussed. Other approaches for absolute X-ray intensity measurement utilizing imaging plates, a dose-measuring medium, have been proposed and discussed in the context of an exploratory study.

We are grateful to Andrew W. Stevenson and Tim Davis for advice and the use of the CSIRO imaging plate and readout system. ZB is grateful to the Australia Research Council for grants supporting the work with extended-face crystals. This work was supported by the Australian Synchrotron Research Program, which is funded by the Commonwealth of Australia under the Major National Research Facilities Program and by a number of grants of the Australia Research Council. Use of the Advanced Photon Source was supported by the US Department of Energy, Basic Energy Sciences, Office of Energy Research, under contract No. W-31-109-Eng-38. We are grateful for the assistance of the synchrotron staff at the Australian National Beamline Facility, at beamline 20B of the Photon Factory in Tsukuba, Japan.

References

- Barnea, Z., Chantler, C. T., de Jonge, M. D., Stevenson, A. W. & Tran, C. Q. (2010). In *Celebration of K. C. Hines*, edited by B. H. J. McKellar & K. Amos, ch. 3, pp. 35–45. Singapore: World Scientific.
- Barnea, Z. & Mohyla, J. (1974). *J. Appl. Cryst.* **7**, 298–299.
- Beaumont, J. H. & Hart, M. (1974). *J. Phys. E*, **7**, 823–829.
- Becker, P. J. & Coppens, P. (1974*a*). *Acta Cryst.* **A30**, 129–147.
- Becker, P. J. & Coppens, P. (1974*b*). *Acta Cryst.* **A30**, 148–153.
- Bonse, U., Materlik, G. & Schröder, W. (1976). *J. Appl. Cryst.* **9**, 223–230.
- Bragg, W. L. & Bragg, W. H. (1962). *The Crystalline State*, p. 29. London: Bell.
- Bragg, W. L. & West, J. (1928). *Z. Kristallogr.* **69**, 118–125.
- Chantler, C. T. (1992*a*). *J. Appl. Cryst.* **25**, 674–693.
- Chantler, C. T. (1992*b*). *J. Appl. Cryst.* **25**, 694–713.
- Chantler, C. T. (1993). *Appl. Opt.* **32**, 2371–2397.
- Chantler, C. T. (1995*a*). *J. Phys. Chem. Ref. Data*, **29**, 597–1056.
- Chantler, C. T. (1995*b*). *J. Phys. Chem. Ref. Data*, **24**, 71–643.
- Chantler, C. T., Laming, J. M., Dietrich, D. D., Hallett, W. A., McDonald, R. & Silver, J. D. (2007). *Phys. Rev. A*, **76**, 042116.
- Chantler, C. T., Laming, J. M., Silver, J. D., Dietrich, D. D., Mokler, P. H., Finch, E. C. & Rosner, S. D. (2009). *Phys. Rev. A*, **80**, 022508.
- Chantler, C. T., Silver, J. D. & Dietrich, D. D. (1993). *Appl. Opt.* **32**, 2411–2421.
- Chantler, C. T. & Staudenmann, J.-L. (1995). *Rev. Sci. Instrum.* **66**, 1651–1654.

- Chantler, C. T., Tran, C. Q., Paterson, D., Barnea, Z. & Cookson, D. J. (2001). *Rad. Phys. Chem.* **61**, 347–350.
- Cookson, D. J. (1998). *J. Synchrotron Rad.* **5**, 1375–1382.
- Creagh, D. C. (1999). *International Tables for Crystallography*, Vol. C, edited by A. J. C. Wilson & E. Prince, pp. 230–232. Dordrecht: Kluwer Academic.
- Dozier, C. M., Gilfrich, J. V. & Birks, L. S. (1967). *Appl. Opt.* **6**, 2136–2139.
- Glover, J. L., Chantler, C. T., Barnea, Z., Rae, N. A., Tran, C. Q., Creagh, D. C., Paterson, D. & Dhal, B. B. (2008). *Phys. Rev. A*, **78**, 052902.
- Grigg, M. W. (1994). PhD thesis, The University of Melbourne, Australia.
- Grigg, M. W. & Barnea, Z. (1996). *J. Appl. Cryst.* **29**, 105–109.
- Harada, J., Pedersen, T. & Barnea, Z. (1970). *Acta Cryst.* **A26**, 336–344.
- Henke, B. L., Kwok, S. L., Uejio, J. Y., Yamada, H. T. & Young, G. C. (1984). *J. Opt. Soc. Am. B*, **1**, 818–827.
- Islam, M. T., Rae, N. A., Glover, J. L., Barnea, Z., de Jonge, M. D., Tran, C. Q., Wang, J. & Chantler, C. T. (2010). *Phys. Rev. A*, **81**, 022903.
- James, R. W. (1962). *The Optical Principles of the Diffraction of X-rays*, p. 44. London: Bell.
- Jonge, M. D. de, Barnea, Z., Tran, C. Q. & Chantler, C. T. (2004). *Meas. Sci. Technol.* **15**, 1811–1822.
- Jonge, M. D. de, Tran, C. Q., Chantler, C. T., Barnea, Z., Dhal, B. B., Cookson, D. J., Lee, W.-K. & Mashayekhi, A. (2005). *Phys. Rev. A*, **71**, 032702.
- Jonge, M. D. de, Tran, C. Q., Chantler, C. T., Barnea, Z., Dhal, B. B., Paterson, D., Kanter, E. P., Southworth, S. H., Young, L., Beno, M. A., Linton, J. A. & Jennings, G. (2007). *Phys. Rev. A*, **75**, 032702.
- Lipson, H. & Cochran, W. (1957). *The Determination of Crystal Structures*, p. 132. London: Bell.
- Mair, S. L., Prager, P. & Barnea, Z. (1971). *Nat. Phys. Sci.* **234**, 35–36.
- McIntyre, G. J. (1981). *Acta Cryst.* **A37**, 105–119.
- McIntyre, G. J., Moss, G. & Barnea, Z. (1980). *Acta Cryst.* **A36**, 482–490.
- Miyahara, J., Takahashi, K., Amemiya, Y., Kamiya, N. & Satow, Y. (1986). *Nucl. Instrum. Methods Phys. Res. Sect. A*, **246**, 572–578.
- Paterson, D., Allman, B. E., McMahon, P. J., Lin, J., Moldovan, N., Nugent, K. A., McNulty, I., Chantler, C. T., Retsch, C. C., Irving, T. H. K. & Mancini, D. C. (2001). *Opt. Commun.* **195**, 79–84.
- Payne, A. T., Kimpton, J. A., Kinnane, M. N. & Chantler, C. T. (2009). *Meas. Sci. Technol.* **20**, 025601.
- Payne, A. T., Kimpton, J. A., Smale, L. F. & Chantler, C. T. (2010). *Nucl. Instr. Methods Phys. Res. Sect. A*, **619**, 190–197.
- Rae, N. A., Chantler, C. T., Barnea, Z., de Jonge, M. D., Tran, C. Q. & Hester, J. R. (2010). *Phys. Rev. A*, **81**, 022904.
- Stevenson, A. W. (1994). *Acta Cryst.* **A50**, 621–632.
- Stevenson, A. W. & Barnea, Z. (1983a). *Acta Cryst.* **A39**, 538–547.
- Stevenson, A. W. & Barnea, Z. (1983b). *Acta Cryst.* **A39**, 548–552.
- Stevenson, A. W. & Barnea, Z. (1984). *Acta Cryst.* **B40**, 530–537.
- Stevenson, A. W., Milanko, M. & Barnea, Z. (1984). *Acta Cryst.* **B40**, 521–530.
- Tran, C. Q., Chantler, C. T., Barnea, Z. & de Jonge, M. D. (2004). *Rev. Sci. Instrum.* **75**, 2943–2949.
- Tran, C. Q., Chantler, C. T., Barnea, Z., Paterson, D. & Cookson, D. J. (2003). *Phys. Rev. A*, **67**, 42716.
- Tran, C. Q., de Jonge, M. D., Barnea, Z. & Chantler, C. T. (2004). *J. Phys. B*, **37**, 3163–3176.
- Warren, B. E. (1969). *X-ray Diffraction*. Reading: Addison-Wesley.
- Zachariasen, W. H. (1967). *Acta Cryst.* **23**, 558–564.